

Asymptotics of Wigner $3nj$ -symbols with Small and Large Angular Momenta: an Elementary Method

Valentin Bonzom^{1,*} and Pierre Fleury^{1,†}

¹*Perimeter Institute for Theoretical Physics, 31 Caroline St. N, ON N2L 2Y5, Waterloo, Canada*

(Dated: February 17, 2022)

Yu and Littlejohn recently studied in arXiv:1104.1499 some asymptotics of Wigner symbols with some small and large angular momenta. They found that in this regime the essential information is captured by the geometry of a tetrahedron, and gave new formulae for $9j$, $12j$ and $15j$ -symbols. We present here an alternative derivation which leads to a simpler formula, based on the use of the Ponzano-Regge formula for the relevant tetrahedron. The approach is generalized to Wigner $3nj$ -symbols with some large and small angular momenta, where more than one tetrahedron is needed, leading to new asymptotics for Wigner $3nj$ -symbols. As an illustration, we present $15j$ -symbols with one, two and four small angular momenta, and give an alternative formula to Yu's recent $15j$ -symbol with three small spins.

INTRODUCTION

Wigner symbols are re-coupling coefficients of $SU(2)$ representation theory. As such they naturally arise when dealing with sums of more than four spins and/or angular momenta in quantum mechanics, and are notoriously important in spectroscopy and atomic/molecular physics. Moreover, they also enter different parts of physics [1], like quantum computing [2] (in the presence of topological order, and mainly with a quantum group deformation [3]), and are expected to contain relevant aspects of quantum geometry (in loop quantum gravity and spin foam models [4–7]).

Although those objects are easily defined, using sums of Clebsch-Gordan coefficients, or inner products of wavefunctions, it is quite hard to extract their semi-classical behavior, for large angular momenta (not even to mention getting a rigorous proof). Moreover, in the typical case of spin-orbit couplings, one may be interested into large angular momenta coupled to some intrinsic spins which cannot be scaled. Obviously, different behaviors are expected in those different regimes of a given symbol.

The most studied Wigner symbol is the $6j$ -symbol, whose asymptotics is known when all spins are large (the Ponzano-Regge formula, [11–14]), or with one being small (the Edmonds' formula [15, 16]). Over the years, the $6j$ -symbol has turned out to be an interesting topic in modern physics, see [17] which contains additional references. Very recent progress include sub-leading corrections to its Ponzano-Regge asymptotics [18–20], a new recursion relation on the square of the $6j$ -symbol [21] and a derivation of its standard recursion relation as a Wheeler-DeWitt equation for three-dimensional Riemannian gravity [22].

When all angular momenta are large, a nice feature of the Ponzano-Regge asymptotics is that all the information is captured into a tetrahedron whose edge lengths are basically the six quantum angular momenta. Such a simple geometric interpretation is usually not available for larger symbols, which makes their analysis more difficult. While a new approach was recently proposed in [23] to classify the various asymptotic regimes of Wigner $3nj$ -symbols, it remains an open issue. In contrast with the generic case, it is interesting to note that the $15j$ -symbol admits a natural four-dimensional interpretation in the coherent state basis, in term of the geometry of a 4-simplex [24, 25] (the same method has been applied to the three-dimensional Ponzano-Regge model, see [26]). Just like for the $6j$ -symbol, that geometric property can be understood via the recursions satisfied by the $15j$ -symbol which naturally arise as Hamiltonian equations for the quantum 4-simplex [27].

Littlejohn and Yu [8] have recently obtained a new formula for the asymptotics of the $9j$ -symbol with eight large angular momenta and one small spin (and also for larger symbols, but the method there focuses on this example, and we will do the same here). Their method is quite generic and powerful since it relies on previous works of the authors which extend the Born-Oppenheimer approximation in the case the fast degrees of freedom are coupled through a matrix of non-commuting operators. We refer the reader to [8] for further references to the method and its applications, as we will be more interested in the asymptotics of the $9j$ -symbol itself.

The asymptotic formula itself is indeed quite interesting. The information is encoded into the geometry of a tetrahedron, and can be re-formulated more conveniently with three tetrahedra. The formula also displays ingredients

* vbonzom@perimeterinstitute.ca

† pierre.fleury@ens-lyon.fr

which are familiar to the asymptotics of the 6j-symbol, as noticed by the authors of [8], more precisely the amplitude involving the inverse of the square-root of the volume of the tetrahedron, and oscillations with part of the frequency given by the Regge action of the same tetrahedron.

This suggests that the asymptotic formula for the 9j-symbol with a small spin may really be derived using the Ponzano-Regge asymptotic formula for some 6j-symbol associated to the relevant tetrahedron. This is exactly what we show in the present paper, ending up with a quite straightforward derivation. Remarkably, not only the derivation but also the final formula turns out to be simpler than that presented in [8]. The Section I is devoted to showing this.

Our analysis further reveals the conditions so that an arbitrary Wigner symbol can be semi-classically described by a number of tetrahedra, when some spins remain small. This way we obtain generic asymptotic formulae for Wigner symbols, presented in the Section II.

As an illustration, we show the formulae for 15j-symbols in the Section III since they may have some interesting applications in four-dimensional models for gravity. The cases with one, two and four small angular momenta are new. The case with three small angular momenta is an alternative to the recent result of [10] and our formula is a bit simpler since all quantities can be evaluated using only two tetrahedra. It should be noted that the method used in [8–10] is surely quite powerful since it has given access to some regimes which cannot be probed with our method. So at the end of the day, we think that both methods yield complementary results, with some overlap, and open an interesting window towards new asymptotics of re-coupling coefficients.

I. ASYMPTOTICS OF THE 9J-SYMBOL WITH ONE SMALL ANGULAR MOMENTUM

A. Notations

We have tried to use as often as possible the same notations as [8]. The large angular momenta, or spins in the sense of irreducible $SU(2)$ representations, are denoted like $j \in \mathbb{N}/2$, and the small spins like $s \in \mathbb{N}/2$.

However, differences appear regarding angles. We systematically call $\varphi_{a,b}$ the (internal) angle between two edges a, b of a triangle. Its value is given in terms of the lengths of the triangle,

$$\cos \varphi_{a,b} = \frac{\ell_a^2 + \ell_b^2 - \ell_c^2}{2 \ell_a \ell_b}, \quad (1)$$

where the third length ℓ_c will be mentioned when necessary.

Lengths are simple functions of spins which will be attached to the corresponding edges,

$$\ell_a \stackrel{\text{def.}}{=} j_a + \frac{1}{2} \stackrel{\text{def.}}{=} d_{j_a}/2. \quad (2)$$

This is the relation which is necessary for the Ponzano-Regge formula to work. But note that when using Edmonds' formula (given explicitly later), those dihedral angles are more naturally given in terms of different lengths $\sqrt{j_a(j_a + 1)}$. The latter are asymptotically equivalent to ℓ_a and the difference in Edmonds' formula only appears at sub-leading orders. Note also that d_j is the dimension of the representation of spin j .

We denote respectively Θ_e and θ_e the external and internal dihedral angles between two triangles adjacent to the edge e in a tetrahedron, with $\Theta_e = \pi - \theta_e$. They are obviously determined by the lengths, and satisfy the following relation

$$\cos \theta_a = \frac{\cos \varphi_{b,c} - \cos \varphi_{a,b} \cos \varphi_{a,c}}{\sin \varphi_{a,b} \sin \varphi_{a,c}}, \quad (3)$$

when the edges a, b, c meet at a node in a tetrahedron.

B. The formula

The 9j-symbol comes as a recoupling coefficient, i.e. a change of basis, when describing in different ways the rotational invariant subspace of a tensor product of five spins¹, say $j_1 \otimes j_2 \otimes s \otimes j_4 \otimes j_5$. The invariant subspace is characterized by the fact that the sum of the angular momenta vanishes,

$$\mathbf{J}_1 + \mathbf{J}_2 + \mathbf{S} + \mathbf{J}_4 + \mathbf{J}_5 = \mathbf{0}. \quad (4)$$

¹ It is actually equivalent to look at the projection of $j_1 \otimes j_2 \otimes s \otimes j_4$ onto the spin j_5 .

A first basis is obtained by choosing a spin j_{13} in the tensor product $j_1 \otimes s$, a spin j_{24} in $j_2 \otimes j_4$, and then consider the unique (normalized) vector satisfying $\mathbf{J}_{13} + \mathbf{J}_{24} + \mathbf{J}_5 = \mathbf{0}$ in $j_{13} \otimes j_{24} \otimes j_5$. Denote this vector $|(j_1, s, j_{13}), j_5, (j_2, j_4, j_{24})\rangle$. An equivalent basis is obtained by tensoring first j_1 with j_2 and choosing a spin j_{12} in the decomposition, and similarly choosing a spin j_{34} in $s \otimes j_4$. A basis vector is then formed by the unique vector satisfying $\mathbf{J}_{12} + \mathbf{J}_{34} + \mathbf{J}_5 = \mathbf{0}$, and is denoted $|(j_1, j_2, j_{12}), j_5, (s, j_4, j_{34})\rangle$. The 9j-symbol is just

$$\langle (j_1, j_2, j_{12}), j_5, (s, j_4, j_{34}) | (j_1, s, j_{13}), j_5, (j_2, j_4, j_{24}) \rangle = [d_{j_{12}} d_{j_{34}} d_{j_{13}} d_{j_{24}}]^{1/2} \begin{Bmatrix} j_1 & j_2 & j_{12} \\ s & j_4 & j_{34} \\ j_{13} & j_{24} & j_5 \end{Bmatrix}, \quad (5)$$

where the normalization is a product of dimensions, $d_j \stackrel{\text{def.}}{=} 2j + 1$.

The asymptotics when all spins are homogeneously scaled is given for instance in [28].

The result of [8] is an asymptotic formula for the 9j-symbol with one spin, s , being small (i.e. not scaled) while the other eight spins are homogeneously scaled by a large number. We will prove here an equivalent but different formula in that case. While the relevant quantities in the formula of [8] need three tetrahedra, all of them are here contained in only two tetrahedra. It is the following

$$\begin{Bmatrix} j_1 & j_2 & j_{12} \\ s & j_4 & j_{34} \\ j_{13} & j_{24} & j_5 \end{Bmatrix} \approx \frac{(-1)^{j_{13}+j_2+j_{34}+j_5+s}}{\sqrt{d_{j_1} d_{j_{34}} (12\pi V_1)}} \cos \left[\sum_{e \subset \text{tet}_1} \left(j_e + \frac{1}{2} \right) \Theta_e^{(1)} + \frac{\pi}{4} - \mu(\pi - \theta_1^{(2)}) - \nu \theta_{34}^{(2)} \right] d_{\mu\nu}^{(s)}(\pi - \varphi_{1,34}). \quad (6)$$

In the above expression,

- the sum in the cosine runs over the six large angular momenta $\{j_e\}_e$ with $e = 1, 2, 34, 5, 12, 24$;
- $\mu \stackrel{\text{def.}}{=} j_{13} - j_1$ and $\nu \stackrel{\text{def.}}{=} j_{34} - j_4$, those two differences have the same order of magnitude as s , due to the triangle inequalities (or Clebsch-Gordan conditions) between the spins (j_1, s, j_{13}) and also between (s, j_4, j_{34}) ;
- V_1 and $\{\Theta_e^{(1)}\}_{e=1,2,34,5,12,24}$ are geometric quantities associated to tetrahedron tet_1 in Figure 1, V_1 is the volume of the tetrahedron and $\Theta_e^{(1)}$ is the angle between two external normals to the faces adjacent to the edge e (external dihedral angle);
- $\varphi_{1,34}$ is associated with the tetrahedron tet_2 given in the Figure 1, it is the angle between the edges 1 and 34; $\theta_1^{(2)}$ and $\theta_4^{(2)}$ are respectively the internal dihedral angles between the faces adjacent to the edges 1 and 34 in tet_2 .
- $d^{(s)}$ is the Wigner d -matrix with spin s , with the convention $d_{\mu\nu}^{(s)}(\phi) = \langle s, \mu | e^{-\frac{i}{2}\phi\sigma_y} | s, \nu \rangle$.

The formula holds in the classically allowed region away from the caustic, i.e. where the volume V_1 of the tetrahedron tet_1 is not close to zero.

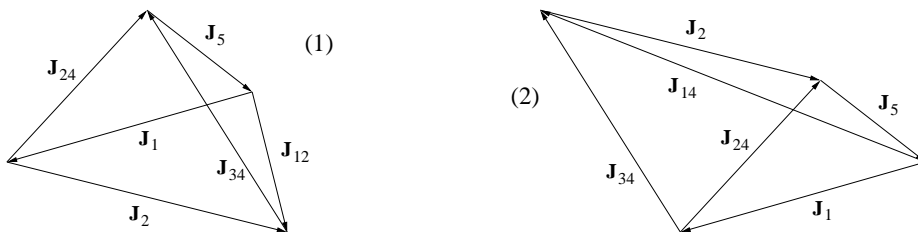


FIG. 1. Tetrahedron tet_1 on the left, constructed with the six lengths $\{j_e + 1/2\}_{e=1,2,34,5,12,24}$, whose faces are the triads $(1, 2, 12)$, $(2, 34, 24)$, $(34, 5, 12)$ and $(1, 5, 24)$. We call \mathbf{J}_e the vector associated with the edge e . Their orientations are such that $\mathbf{J}_{12} = \mathbf{J}_1 + \mathbf{J}_2$, $\mathbf{J}_{24} = \mathbf{J}_2 + \mathbf{J}_{34}$, and $\mathbf{J}_{34} + \mathbf{J}_5 + \mathbf{J}_{12} = \mathbf{J}_1 + \mathbf{J}_5 + \mathbf{J}_{24} = \mathbf{0}$. Tetrahedron tet_2 on the right is constructed from the vectors $\mathbf{J}_1, \mathbf{J}_2, \mathbf{J}_{34}, \mathbf{J}_5, \mathbf{J}_{24}$. The last vector \mathbf{J}_{14} is simply the sum $\mathbf{J}_1 + \mathbf{J}_{34}$.

The tetrahedron tet_2 is built by gluing the triangles $(2, 34, 24)$ and $(1, 5, 24)$ along 24, similarly to tetrahedron tet_1 , but after flipping one of the triangles. This means that 2 and 5 meet at one end of 24, and 1 and 34 meet at the other node. To completely determine tet_2 , one has to set the dihedral angle between the two triangles. It is $\theta_{24}^{(2)} = \Theta_{24}^{(1)}$. This can be deduced, like in [8], from the vectors representing the classical angular momenta, which are drawn on the Figure 1. This is indeed equivalent to adding to tet_1 the parallelogram spanned by $\mathbf{J}_2, \mathbf{J}_{34}$, and observe that tet_2 is

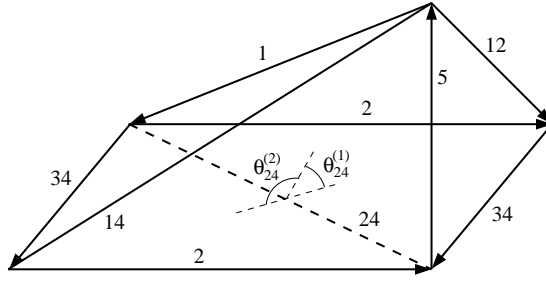


FIG. 2. That is a unified view of the two relevant tetrahedra tet_1 and tet_2 . They form a pyramid with a parallelogram basis spanned by $\mathbf{J}_2, \mathbf{J}_{34}$. Without using the vectors, one can define tet_2 by setting the angle $\theta_{34}^{(2)} = \pi - \theta_{34}^{(1)}$, which is obvious in the picture, and that makes it possible to evaluate the additional length j_{14} .

the tetrahedron between the parallelogram and tet_1 . That observation is summarized in the Figure 2 which offers a full view on the two relevant tetrahedra.

Our tetrahedra are closely related to those used in [8]. Their first tetrahedron is like ours but with \mathbf{J}_4 instead of \mathbf{J}_{34} (notice indeed that they differ only by a vector of order s). Their second tetrahedron is built just like tet_2 from tet_1 . Because we are using a different first tetrahedron, the Regge action $\sum_{e \in \text{tet}_1} (j_e + \frac{1}{2}) \Theta_e^{(1)}$ in the cosine is not the same. The difference, which can be observed in [8], is a term $\nu \Theta_{34}^{(1)}$. This adds to the explicit ν contribution in (6), which becomes $\nu(\Theta_{34}^{(1)} - \theta_{34}^{(2)})$. That new angle can be interpreted with the introduction of a third tetrahedron, which is the additional tetrahedron of [8].

C. Direct derivation of the formula

Our derivation starts from a decomposition² of the 9j-symbol in terms of 6j-symbols [28]

$$\left\{ \begin{matrix} j_1 & j_2 & j_{12} \\ s & j_4 & j_{34} \\ j_{13} & j_{24} & j_5 \end{matrix} \right\} = \sum_x (-1)^{2x} d_x \left\{ \begin{matrix} j_1 & j_2 & j_{12} \\ j_{34} & j_5 & x \end{matrix} \right\} \left\{ \begin{matrix} s & j_4 & j_{34} \\ j_2 & x & j_{24} \end{matrix} \right\} \left\{ \begin{matrix} j_{13} & j_{24} & j_5 \\ x & j_1 & s \end{matrix} \right\}. \quad (7)$$

The range of summation of x is finite due to triangle inequalities. x is bounded from below by $\max(|j_{24} - s|, |j_1 - j_5|, |j_2 - j_{34}|)$, and from above by $\min(j_{24} + s, j_1 + j_5, j_2 + j_{34})$. Now the regime we are looking at, away from the caustic where the volume of tet_1 becomes close to zero, ensures that neither $\max(|j_1 - j_5|, |j_2 - j_{34}|)$ nor $\min(j_1 + j_5, j_2 + j_{34})$ are close to j_{24} up to terms of order s . Hence, from the non-degeneracy of tet_1 , we know that x runs from $j_{24} - s$ to $j_{24} + s$. Introduce $\xi \stackrel{\text{def.}}{=} x - j_{24}$ which lives in $\{-s, \dots, s\}$, and write $j_{13} = j_1 + \mu$, $j_{34} = j_4 + \nu$. Then,

$$\left\{ \begin{matrix} j_1 & j_2 & j_{12} \\ s & j_4 & j_{34} \\ j_{13} & j_{24} & j_5 \end{matrix} \right\} = \sum_{\xi=-s}^s d_{j_{24}+\xi} (-1)^{2j_{24}+2s} \left\{ \begin{matrix} s & j_{34} - \nu & j_{34} \\ j_2 & j_{24} + \xi & j_{24} \end{matrix} \right\} \left\{ \begin{matrix} j_1 + \mu & j_{24} & j_5 \\ j_{24} + \xi & j_1 & s \end{matrix} \right\} \left\{ \begin{matrix} j_1 & j_2 & j_{12} \\ j_{34} & j_5 & j_{24} + \xi \end{matrix} \right\}. \quad (8)$$

We observe that there are two different situations for the above 6j-symbols. The last one does not contain s , so that its large spin behavior is given by the Ponzano-Regge formula. The other two 6j-symbols only have five large spins, and their asymptotics are given by Edmonds' formula.

The presence of the symbol $\left\{ \begin{matrix} j_1 & j_2 & j_{12} \\ j_{34} & j_5 & j_{24} + \xi \end{matrix} \right\}$ in (8) will make clear why the geometry of the tetrahedron tet_1 is important. It is indeed well known that the asymptotics of that symbol is described using a tetrahedron geometry, with oscillations following the Regge action for that tetrahedron. Precisely,

$$\left\{ \begin{matrix} j_1 & j_2 & j_{12} \\ j_{34} & j_5 & j_{24} + \xi \end{matrix} \right\} \approx \frac{\cos(S_R(\xi) + \frac{\pi}{4})}{\sqrt{12\pi V(\xi)}}. \quad (9)$$

² There are several such decompositions. Those we are interested in are such that the summed variable, here x , has to satisfy Clebsch-Gordan conditions with the small spin s . There are four such possibilities. In our choice, j_{24} will play a special role in the following. But we could have equally well chosen j_2, j_{12} or j_{34} instead.

$V(\xi)$ and $S_R(\xi)$ are the volume and the Regge action of the tetrahedron constructed with the lengths $j_1 + 1/2$, $j_2 + 1/2$, $j_{12} + 1/2$, $j_{34} + 1/2$, $j_5 + 1/2$, $j_{24} + \xi + 1/2$, in such a way that the triangles are formed by the spins which are coupled in the $6j$ -symbol (through Clebsch-Gordan couplings). Since that tetrahedron differs from the tetrahedron tet_1 only due to a small ξ of order s along the vector \mathbf{J}_{24} , one can relate $S_R(\xi)$ to the Regge action $S_R^{(1)}$ of tetrahedron tet_1 via

$$S_R(\xi) \approx S_R^{(1)} + \xi \Theta_{24}^{(1)}, \quad \text{with} \quad S_R^{(1)} \stackrel{\text{def.}}{=} \sum_{e \in \text{tet}_1} \left(j_e + \frac{1}{2} \right) \Theta_e^{(1)}. \quad (10)$$

Here, the difference between the dihedral angles $\Theta_e(\xi)$ appearing in $S_R(\xi)$ and the dihedral angles $\Theta_e^{(1)}$ of tet_1 have been omitted thanks to the Schläfli's identity (it makes sure that those sum to zero on the six edges of the tetrahedron). Besides, the variations of V with ξ are irrelevant at the leading order, so that $V(\xi) \approx V_1$.

The other two $6j$ -symbols can be expressed using Edmonds' formula³ [28]:

$$\left\{ \begin{matrix} s & j_{34} - \nu & j_{34} \\ j_2 & j_{24} + \xi & j_{24} \end{matrix} \right\} \approx \frac{(-1)^{j_2 + j_{24} + j_{34} + s}}{\sqrt{d_{j_{34}} d_{j_{24}}}} d_{-\xi - \nu}^{(s)}(\varphi_{34,24}), \quad (11)$$

$$\left\{ \begin{matrix} j_1 + \mu & j_{24} & j_5 \\ j_{24} + \xi & j_1 & s \end{matrix} \right\} \approx \frac{(-1)^{j_{13} + j_{24} + j_5} (-1)^{s + \xi}}{\sqrt{d_{j_1} d_{j_{24}}}} d_{\mu - \xi}^{(s)}(\varphi_{1,24}). \quad (12)$$

We use symmetries of the Wigner matrices to write $d_{-\xi - \nu}^{(s)}(\varphi_{34,24}) = (-1)^{s - \xi} d_{-\xi \nu}^{(s)}(\pi - \varphi_{34,24})$. Inserting those asymptotics in (8) and relabeling the sum by $\xi \mapsto -\xi$, we get

$$\{9j\} \approx \frac{(-1)^{j_{13} + j_2 + j_{34} + j_5 + s}}{\sqrt{d_{j_1} d_{j_{34}}} (12\pi V_1)} \sum_{\xi = -s}^s \cos\left(S_R^{(1)} + \frac{\pi}{4} - \xi \Theta_{24}^{(1)}\right) d_{\mu \xi}^{(s)}(\varphi_{1,24}) d_{\xi \nu}^{(s)}(\pi - \varphi_{34,24}), \quad (13)$$

The sum over ξ is almost a matrix product between the two Wigner d -matrices, but not exactly because the argument of the cosine does depend on ξ . Nevertheless the sum over ξ is a matrix product of Wigner D -matrices. To see that, we simply write the cosine as a sum of exponentials. Let us call A the prefactor of the sum. We get the following expression

$$\{9j\} \approx A e^{i(S_R^{(1)} + \pi/4)} \sum_{\xi = -s}^s d_{\mu \xi}^{(s)}(\varphi_{1,24}) e^{-i\xi \Theta_{24}^{(1)}} d_{\xi \nu}^{(s)}(\pi - \varphi_{34,24}) + \text{c.c.}, \quad (14)$$

where 'c.c.' denotes the complex conjugate of the whole expression. By definition of the Wigner D -matrices, the sum can then be re-expressed as a matrix product,

$$\sum_{\xi} d_{\mu \xi}^{(s)}(\varphi_{1,24}) e^{-i\xi \Theta_{24}^{(1)}} d_{\xi \nu}^{(s)}(\pi - \varphi_{34,24}) = D_{\mu \nu}^{(s)} \left(e^{-i\varphi_{1,24} \frac{\sigma_y}{2}} e^{-i\Theta_{24}^{(1)} \frac{\sigma_z}{2}} e^{-i(\pi - \varphi_{34,24}) \frac{\sigma_y}{2}} \right). \quad (15)$$

We have used above the notation in terms of $\text{SU}(2)$ rotations, written with the Pauli matrices as generators. The last step of the calculation is to rewrite the relevant product of rotations as a single rotation parametrized by its Euler angles⁴. That rewriting, from the angles $\varphi_{1,24}$, $\Theta_{24}^{(1)}$, $\varphi_{34,24}$ to Euler angles, will naturally be encoded into the geometry of the tetrahedron tet_2 . Explicitly, we define three new angles $\theta_1^{(2)}$, $\varphi_{1,34}$, $\theta_{34}^{(2)}$ by

$$e^{-i\varphi_{1,24} \frac{\sigma_y}{2}} e^{-i\Theta_{24}^{(1)} \frac{\sigma_z}{2}} e^{-i(\pi - \varphi_{34,24}) \frac{\sigma_y}{2}} = e^{-i(\pi - \theta_1^{(2)}) \frac{\sigma_z}{2}} e^{-i(\pi - \varphi_{1,34}) \frac{\sigma_y}{2}} e^{-i\theta_{34}^{(2)} \frac{\sigma_z}{2}}. \quad (16)$$

The relation between both sets can be found in textbooks like [28]. Since all our angles lie in $[0, \pi]$, we can simply make use of the $\text{SO}(3)$ relations,

$$\begin{aligned} \cos \varphi_{1,34} &= \cos \varphi_{1,24} \cos \varphi_{34,24} + \sin \varphi_{1,24} \sin \varphi_{34,24} \cos \Theta_{24}^{(1)}, \\ \cos \theta_{34}^{(2)} &= \frac{\cos \varphi_{1,24} - \cos \varphi_{34,24} \cos \varphi_{1,34}}{\sin \varphi_{34,24} \sin \varphi_{1,34}}, \quad \cos \theta_1^{(2)} = \frac{\cos \varphi_{34,24} - \cos \varphi_{1,24} \cos \varphi_{1,34}}{\sin \varphi_{1,24} \sin \varphi_{1,34}}, \\ \frac{\sin \theta_1^{(2)}}{\sin \varphi_{34,24}} &= \frac{\sin \theta_{34}^{(2)}}{\sin \varphi_{1,24}} = \frac{\sin \Theta_{24}^{(1)}}{\sin \varphi_{1,34}}. \end{aligned} \quad (17)$$

³ It gives the asymptotic behavior of a $6j$ -symbol when one spin is much smaller than the five others,

$$\left\{ \begin{matrix} a & b & c \\ b+m & a+n & f \end{matrix} \right\}_{a,b,c \gg m,n,f} \approx \frac{(-1)^{a+b+c+f+m}}{\sqrt{(2a+1)(2b+1)}} d_{mn}^{(f)}(\varphi_{a,b}),$$

where $\varphi_{a,b}$ is the angle between the edges a and b in the triangle constructed with the three lengths ℓ_a , ℓ_b , ℓ_c .

⁴ Our convention for the Euler angles is the form $g = e^{-\frac{1}{2}\alpha\sigma_z} e^{-\frac{1}{2}\beta\sigma_y} e^{-\frac{1}{2}\gamma\sigma_z}$ for $g \in \text{SU}(2)$, together with $\sigma_z = \text{diag}(1, -1)$, $\sigma_y = \begin{pmatrix} 0 & -i \\ i & 0 \end{pmatrix}$.

As our notation suggests, those new angles have a nice geometric interpretation with the help of the tetrahedron tet_2 . The latter appears in the following way. Those equations characterize the relationship between 2d and 3d angles for three triangles forming the ‘top’ of a tetrahedron, as displayed in Figure 3. The initial angles $\varphi_{1,24}, \Theta_{24}^{(1)}, \varphi_{34,24}$ enable to draw three links, 1, 34, 24 meeting at a node, with two 2d angles being $\varphi_{1,24}, \varphi_{34,24}$ and the (internal) angle between the planes (34, 24) and (1, 24) being $\Theta_{24}^{(1)}$. Then the above formulae make it possible to evaluate the three remaining angles. The first equation states that $\varphi_{1,34}$ is the angle between the edges 1 and 34. And $\theta_1^{(2)}, \theta_{34}^{(2)}$ given by the above formulae are the two other internal dihedral angles. Those geometric considerations are summarized in Figure 3. This is exactly the geometry of the ‘top’ of tet_2 , see Figure 1, where 1, 34, 24 meet⁵.

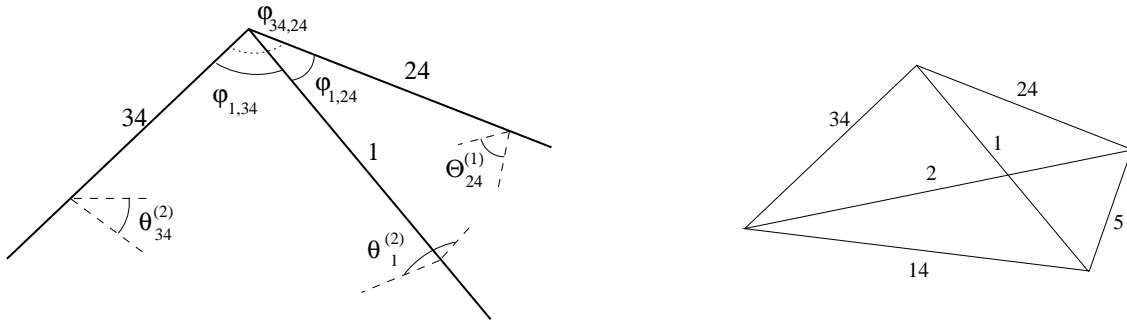


FIG. 3. Geometric interpretation of the Euler angles $\varphi_{1,34}, \theta_1^{(2)}$ and $\theta_{34}^{(2)}$. They appear naturally as characteristics of tetrahedron tet_2 , defined in Figure 1, and re-depicted here on the right.

The element $D_{\mu\nu}^{(s)}$ of the Wigner D-matrix of the relevant $SU(2)$ rotation can then be written in term of the element $d_{\mu\nu}^{(s)}$ of a d -matrix, so that the 9j-symbol takes the following form

$$\{9j\} \approx A \exp \left[i \left(S_R^{(1)} + \frac{\pi}{4} - \mu(\pi - \theta_1^{(2)}) - \nu\theta_{34}^{(2)} \right) \right] d_{\mu\nu}^{(s)}(\pi - \varphi_{1,34}) + \text{c.c.}, \quad (18)$$

that is to say

$$\begin{Bmatrix} j_1 & j_2 & j_{12} \\ s & j_4 & j_{34} \\ j_{13} & j_{24} & j_5 \end{Bmatrix} \approx \frac{(-1)^{j_{13}+j_2+j_{34}+j_5+s}}{\sqrt{d_{j_1} d_{j_{34}}} (12\pi V_1)} \cos \left[S_R^{(1)} + \frac{\pi}{4} - \mu(\pi - \theta_1^{(2)}) - \nu\theta_{34}^{(2)} \right] d_{\mu\nu}^{(s)}(\pi - \varphi_{1,34}). \quad (19)$$

This is exactly the formula (6).

Since our formula is different from that of Yu and Littlejohn, it is worth comparing it directly with numerics. From the derivation, it is clear that our formula holds as long as the Edmonds’ and Ponzano-Regge formulae do. The comparison with the numerically computed 9j-symbol is indeed very good, as it can be seen on the plots of Figure 4. To show that the agreement becomes better at large spins, we used the symbol $\begin{Bmatrix} j_1 + \frac{1}{2} & \frac{201}{2} & j_1 + 3 \\ 1 & 60 & 61 \\ j_1 + \frac{3}{2} & j_{24} & \frac{99}{2} \end{Bmatrix}$, Figure 4(c), for values of j_1 from 63 to 160. For the smallest values of j_1 , the approximation breaks down because the volume of tet_1 becomes negative. The same phenomenon is observed on Figure 4(a) and the error plot 4(b), where the error increases when we reach the low and high values of j_{24} .

Notice that the corresponding symbol is $\begin{Bmatrix} 430 & 30 & 430 \\ 1 & 60 & 61 \\ 431 & j_{24} & 430 \end{Bmatrix}$, whose large spins differ by a factor 10. It means that the approximation is still good when tet_1 is distorted with some large angular momenta larger than other.

II. ASYMPTOTICS OF 3NJ-SYMBOLS WITH SMALL AND LARGE ANGULAR MOMENTA

A. Decomposition of a 3nj-symbol

For $n \geq 4$, there exist several ways to define a 3nj-symbol. For instance, in the case $n = 4$, one can define two different kinds of (irreducible) 12j-symbols. We restrict the discussion to the first kind, in the terminology of [29],

⁵ Note that the edges 2 and 5 are somehow irrelevant here. This means that from the tetrahedron tet_2 only the apex where (1, 34, 24) meet is interesting, while the base triangle formed by 2, 14, 5 does not provide interesting information.

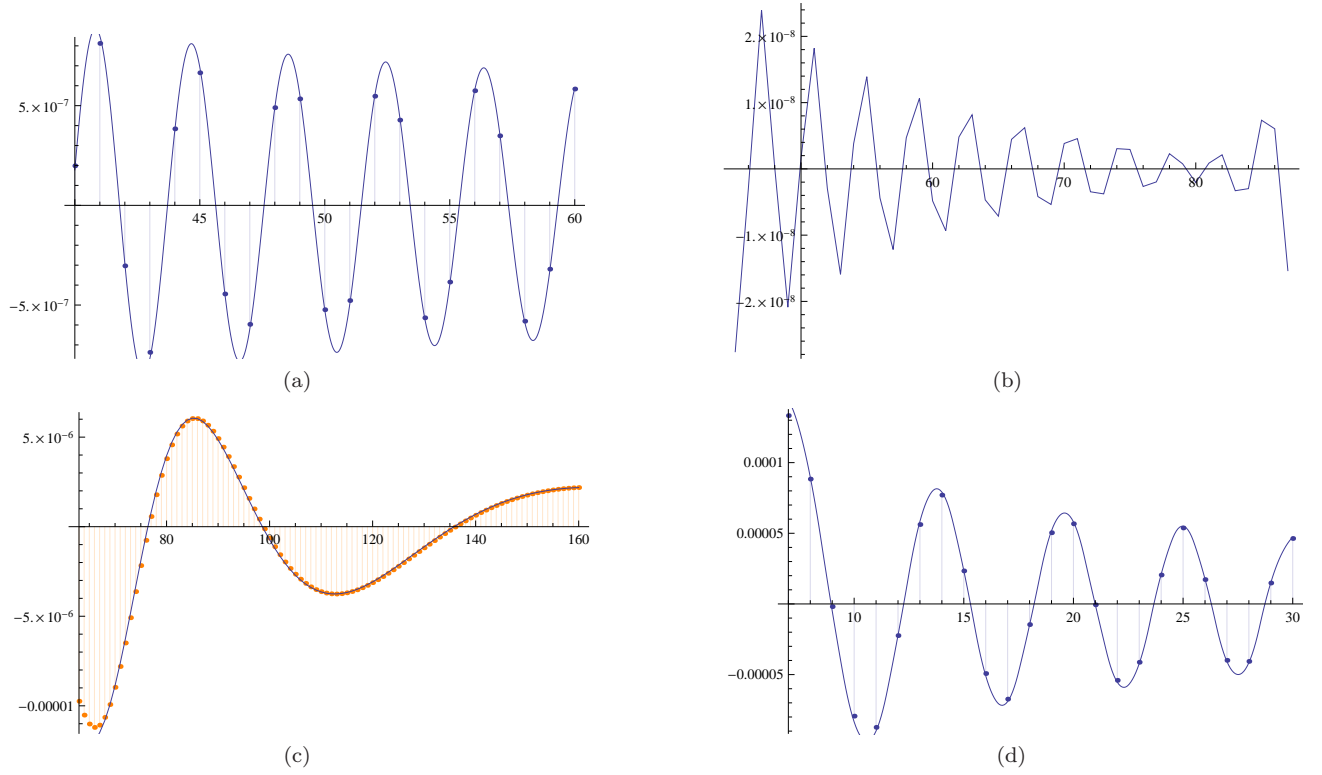


FIG. 4. On 4(a), 4(c), 4(d), the points correspond to the exact 9j-symbols and the curve to the asymptotic formulae. Figure 4(a) is the symbol $\left\{ \begin{matrix} 430 & 30 & 430 \\ 1 & 60 & 61 \\ 431 & j_{24} & 430 \end{matrix} \right\}$ and 4(b) plots the absolute difference between the exact values and the asymptotics. Figure 4(c) plots the symbol $\left\{ \begin{matrix} j_1 + \frac{1}{2} & \frac{201}{2} & j_1 + 3 \\ 1 & 60 & 61 \\ j_1 + \frac{3}{2} & j_{24} & \frac{99}{2} \end{matrix} \right\}$, and Figure 4(d) the symbol $\left\{ \begin{matrix} \frac{51}{2} & \frac{53}{2} & 28 \\ \frac{1}{2} & \frac{47}{2} & 24 \\ 25 & 27 & j_5 \end{matrix} \right\}$.

whose decomposition in terms of 6j-symbols is

$$\left\{ \begin{matrix} j_1 & j_2 & \dots & j_n \\ l_1 & l_2 & \dots & l_n \\ k_1 & k_2 & \dots & k_n \end{matrix} \right\} = \sum_x d_x (-1)^{R_n + (n-1)x} \left\{ \begin{matrix} j_1 & k_1 & x \\ k_2 & j_2 & l_1 \end{matrix} \right\} \left\{ \begin{matrix} j_2 & k_2 & x \\ k_3 & j_3 & l_2 \end{matrix} \right\} \dots \left\{ \begin{matrix} j_{n-1} & k_{n-1} & x \\ k_n & j_n & l_{n-1} \end{matrix} \right\} \left\{ \begin{matrix} j_n & k_n & x \\ j_1 & k_1 & l_n \end{matrix} \right\}, \quad (20)$$

where $R_n \stackrel{\text{def.}}{=} \sum_{i=1}^n j_i + k_i + l_i$. In Equation (20), we wrote the 3nj-symbol so that the coupled spin triads appear easily, namely: (j_1, l_1, j_2) , (j_2, l_2, j_3) , \dots , (j_{n-1}, l_{n-1}, j_n) , (j_n, l_n, k_1) , (k_1, l_1, k_2) , \dots , (k_{n-1}, l_{n-1}, k_n) , (k_n, l_n, j_1) . Those couplings are also fully represented in the involved 6j-symbols.

Symmetries of the 3nj-symbols can be deduced from the symmetries of the 6j-symbols in the above decomposition [28]. It is convenient to distinguish two groups of spins which have different roles, $(j_1, \dots, j_n, k_1, \dots, k_n)$ and (l_1, \dots, l_n) . Then the 3nj-symbol is invariant under simultaneous circular permutations within those groups. It is also invariant under the exchange of the j -row with the k -row.

B. Hypotheses - applicability of the method

Almost all the angular momenta are large, and a few of them can be chosen not to scale. Our method applies when the following conditions are satisfied:

1. *one and only one* spin among $j_1, \dots, j_n, k_1, \dots, k_n$ is small, every other small spin must be an l_i ;
2. we are *away from the caustic*, i.e. the volumes of the tetrahedra associated with the 6j-symbols in (20) which do only have large spins are far from zero.
3. the small l_i must be chosen so that in each 6j-symbol of the decomposition (20), there is *at most one* small spin;

The two first conditions ensure that the summed variable x in (20) is of the order of the large spins, while its range is controlled by the small spin chosen among $(j_1, \dots, j_n, k_1, \dots, k_n)$ ⁶. Precisely, if j_1 is small, then $k_1 - j_1 \leq x \leq k_1 + j_1$. The last restriction enables us to use standard asymptotic expressions of the $6j$ -symbol, the Ponzano-Regge and Edmonds' formulae.

C. Asymptotics of the summand

Without loss of generality (thanks to the symmetries of the symbol) we choose j_1 to be small. Let also $\{l_m\}_{m \in \mathcal{E}}$ be small, for a set of integers $\mathcal{E} \subset \{2, \dots, n-1\}$. We introduce the following half-integers which are small due to the triangular inequalities,

$$\left\{ \begin{array}{l} \xi \stackrel{\text{def.}}{=} x - k_1 \\ \mu \stackrel{\text{def.}}{=} j_2 - l_1 \\ \nu \stackrel{\text{def.}}{=} k_n - l_n \end{array} \right. \quad \text{and} \quad \forall m \in \mathcal{E} \quad \left\{ \begin{array}{l} \eta_m \stackrel{\text{def.}}{=} j_{m+1} - j_m \\ \kappa_m \stackrel{\text{def.}}{=} k_{m+1} - k_m, \end{array} \right. \quad (21)$$

where $\xi, \mu, \nu \in \{-j_1, \dots, j_1\}$ and $\forall m \in \mathcal{E} \quad \eta_m, \kappa_m \in \{-l_m, \dots, l_m\}$. We are now ready to use asymptotic formulae for each $6j$ -symbol involved in (20).

1. $6j$ -symbols with one small spin

Edmonds' formula applies to the $6j$ -symbols with one small spin,

$$\left\{ \begin{array}{ccc} j_1 & k_1 & x \\ k_2 & j_2 & l_1 \end{array} \right\} \approx \frac{(-1)^{(j_1+\mu)+(k_1+k_2+l_1)}}{\sqrt{d_{k_1} d_{l_1}}} d_{\mu\xi}^{(j_1)}(\phi_1), \quad (22)$$

$$\left\{ \begin{array}{ccc} j_n & k_n & x \\ j_1 & k_1 & l_n \end{array} \right\} \approx \frac{(-1)^{(j_1+\xi)+(j_n+l_n+k_1)}}{\sqrt{d_{l_n} d_{k_1}}} d_{\xi\nu}^{(j_1)}(\phi_n), \quad (23)$$

and $\forall m \in \mathcal{E}$

$$\left\{ \begin{array}{ccc} j_m & k_m & x \\ k_{m+1} & j_{m+1} & l_m \end{array} \right\} \approx \frac{(-1)^{(\kappa_m+l_m)+(j_m+k_m+k_1+\xi)}}{\sqrt{d_{j_m} d_{k_m}}} d_{\kappa_m \eta_m}^{(l_m)}(\varphi_m). \quad (24)$$

The angles ϕ_1 , ϕ_n and $(\varphi_m)_{m \in \mathcal{E}}$ are defined geometrically in Figure 5. As we perform all the calculations to the leading order, we can neglect the variations of φ_m with ξ , namely we take k_1 instead of $k_1 + \xi$ for the construction of the triangle $(j_m, k_m, k_1 + \xi)$ in the Figure 5. Also note that $l_1 \approx j_2$ and $l_n \approx k_n$, because j_1 is small.

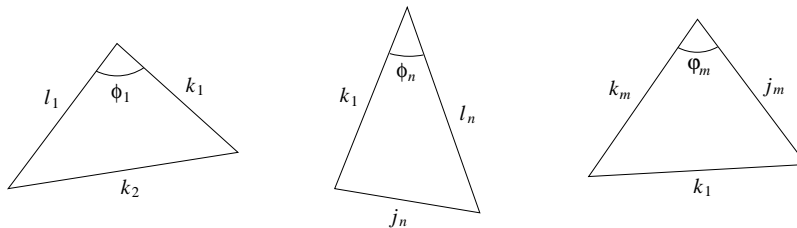


FIG. 5. Definitions of ϕ_1 , ϕ_n and $(\varphi_m)_{m \in \mathcal{E}}$ as angles in triangles. Each edge e is labelled by a spin j_e which indicates its length $\ell_e = \sqrt{j_e(j_e + 1)} \approx j_e + 1/2$.

⁶ In fact, that explains only why we need *at least* one small spin among $(j_1, \dots, j_n, k_1, \dots, k_n)$. The reason why we must have *at most* one appears later. The main idea is to ensure that the sum over x is a product of two Wigner matrices.

2. $6j$ -symbols with six large spins

Let \mathcal{P} be the set of labels p corresponding to $6j$ -symbols with six large spins, namely $\mathcal{P} \stackrel{\text{def.}}{=} \{2, \dots, n-1\} \setminus \mathcal{E}$. We apply the Ponzano-Regge formula to those symbols, and use the same development of the Regge action as in Equation (10) to get for all $p \in \mathcal{P}$

$$\left\{ \begin{matrix} j_p & k_p & x \\ k_{p+1} & j_{p+1} & l_p \end{matrix} \right\} \approx \frac{1}{\sqrt{12\pi V_p}} \cos \left(S_R^{(p)} + \xi \Theta_{k_1}^{(p)} + \frac{\pi}{4} \right), \quad (25)$$

where V_p and $S_R^{(p)}$ are respectively the volume and the Regge action of the tetrahedron tet_p depicted in Figure 6. It is constructed in the usual way from the $6j$ -symbol in the left-hand side (25), for $\xi = 0$.

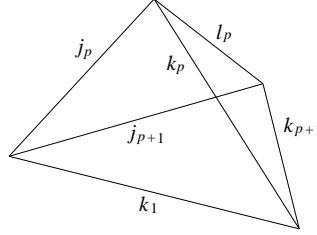


FIG. 6. Tetrahedron tet_p canonically associated with the $6j$ -symbol $\left\{ \begin{matrix} j_p & k_p & k_1 \\ k_{p+1} & j_{p+1} & l_p \end{matrix} \right\}$. Each edge e is labeled by a spin j_e which indicates its length $\ell_e = j_e + 1/2$.

The Regge action $S_R^{(p)}$ of that tetrahedron is explicitly given by $S_R^{(p)} \stackrel{\text{def.}}{=} \sum_{e \subset \text{tet}_p} (j_e + 1/2) \Theta_e^{(p)}$, where $\Theta_e^{(p)}$ is the external dihedral angle at the edge e in tet_p .

D. Evaluation of the sum

Gathering the above pieces into the decomposition (20) of the $3nj$ -symbol, we obtain

$$\begin{aligned} \{3nj\} &\approx \frac{(-1)^{r_n(\mathcal{E})}}{\sqrt{d_{l_1} d_{l_n}}} \left[\prod_{m \in \mathcal{E}} \frac{d_{\kappa_m \eta_m}^{(l_m)}(\varphi_m)}{\sqrt{d_{j_m} d_{k_m}}} \right] \\ &\times \sum_{\xi = -j_1}^{j_1} (-1)^{(n+M)(j_1 - \xi)} d_{\mu\xi}^{(j_1)}(\phi_1) d_{\xi\nu}^{(j_1)}(\phi_n) \prod_{p \in \mathcal{P}} \frac{1}{\sqrt{12\pi V_p}} \cos \left(S_R^{(p)} + \xi \Theta_{k_1}^{(p)} + \frac{\pi}{4} \right), \quad (26) \end{aligned}$$

with $M \stackrel{\text{def.}}{=} |\mathcal{E}|$ and $r_n(\mathcal{E}) \stackrel{\text{def.}}{=} R_n + (n+M-1)(k_1 + j_1) + (\mu - j_1) + (k_1 + k_2 + l_1) + (k_1 + j_n + l_n) + \sum_{m \in \mathcal{E}} j_m + l_m + k_{m+1}$. In practice, we expect that this asymptotic formula can be used numerically. Every angle which is involved has a precise definition in terms of the angular momenta $\{j_i, k_i, l_i\}_i$, and sums and products are finite.

But we can go one step further and recast the sum over ξ as a D -matrix product. That leads to a general asymptotic formula for $3nj$ -symbols, which we do not think is more powerful in terms of numerical computations, but which has a clearer geometric meaning.

As in the case of the $9j$ -symbol, we extract ξ from the argument of the cosines by writing each cosine as a sum of complex exponentials. Expanding the product of cosines and re-organizing its terms, we obtain the following combinatorial expression

$$\prod_{p \in \mathcal{P}} \cos \left(S_R^{(p)} + \xi \Theta_{k_1}^{(p)} + \frac{\pi}{4} \right) = \frac{1}{2^{P+1}} \sum_{\substack{\{\sigma_p = \pm 1, \\ p \in \mathcal{P}\}}} \exp i \left[\sum_{p \in \mathcal{P}} \sigma_p \left(S_R^{(p)} + \frac{\pi}{4} \right) + \xi \sum_{p \in \mathcal{P}} \sigma_p \Theta_{k_1}^{(p)} \right] + \text{c.c.}, \quad (27)$$

where $P \stackrel{\text{def.}}{=} |\mathcal{P}|$ is the number of Ponzano-Regge formulae which we have used. Note that in (27) we have used the symmetry ($\sigma_p \rightarrow -\sigma_p$) of the sum to make the complex conjugation explicit.

We perform the sum over ξ for each configuration $\{\sigma\}$ independently. Since j_1 and ξ may not be integers, we write $(-1)^{(n+M)(j_1-\xi)} = \exp i\pi(n+M)(j_1-\xi)$ and define the angle

$$\omega_{k_1}^{\{\sigma\}} \stackrel{\text{def.}}{=} (n+M)\pi - \sum_{p \in \mathcal{P}} \sigma_p \Theta_{k_1}^{(p)} \pmod{4\pi}. \quad (28)$$

The reason why it is defined only modulo 4π is that generically $j_1 \in \mathbb{N}/2$. The sum over ξ reads

$$\sum_{\xi=-j_1}^{j_1} d_{\mu\xi}^{(j_1)}(\phi_1) e^{-i\xi\omega_{k_1}^{\{\sigma\}}} d_{\xi\nu}^{(j_1)}(\phi_n) = D_{\mu\nu}^{(j_1)}(e^{-\frac{i}{2}\phi_1\sigma_y} e^{-\frac{i}{2}\omega_{k_1}^{\{\sigma\}}\sigma_z} e^{-\frac{i}{2}\phi_n\sigma_y}). \quad (29)$$

Like in the case of the 9j-symbol, the final step is to find the Euler angles of the SU(2) rotation on the right hand side. They have a nice geometric picture as angles of a tetrahedron, but provided ω ranges in an interval of size π (so that it can be a dihedral angle). Since $\omega_{k_1}^{\{\sigma\}}$ is generically in $[-2\pi, 2\pi]$, we distinguish four cases.

1. **Case** $\omega_{k_1}^{\{\sigma\}} \in [0, \pi]$. The formula for the Euler angles show that $\omega_{k_1}^{\{\sigma\}}$ has a natural interpretation as an *external* dihedral angle. So we consider the tetrahedron $\text{tet}_{\{\sigma\}}$ depicted in Figure 7, defined by the gluing of the triangles (k_1, k_n, j_n) and (k_1, l_1, k_2) (which carry the angles ϕ_1 and ϕ_n , see Figure 5) with dihedral angle

$$\theta_{k_1}^{\{\sigma\}} \stackrel{\text{def.}}{=} \pi - \omega_{k_1}^{\{\sigma\}}. \quad (30)$$

It is such that

$$D_{\mu\nu}^{(j_1)}(e^{-\frac{i}{2}\phi_1\sigma_y} e^{-\frac{i}{2}(\pi-\theta_{k_1}^{\{\sigma\}})\sigma_z} e^{-\frac{i}{2}\phi_n\sigma_y}) = e^{-i\mu\theta_{l_1}^{\{\sigma\}}} d_{\mu\nu}^{(j_1)}(\varphi_{l_1, l_n}^{\{\sigma\}}) e^{-i\nu\theta_{l_n}^{\{\sigma\}}}, \quad (31)$$

where the angles are shown on Figure 7 and satisfy the relations (3), (17).

2. **Case** $\omega_{k_1}^{\{\sigma\}} \in [-2\pi, -\pi]$. Then we write

$$\theta_{k_1}^{\{\sigma\}} \stackrel{\text{def.}}{=} -\pi - \omega_{k_1}^{\{\sigma\}}, \quad (32)$$

which is in $[0, \pi]$. Notice that

$$e^{-i\xi\omega_{k_1}^{\{\sigma\}}} = e^{2i\pi\xi} e^{-i(\pi-\theta_{k_1}^{\{\sigma\}})\xi} = e^{2i\pi j_1} e^{-i(\pi-\theta_{k_1}^{\{\sigma\}})\xi}. \quad (33)$$

Hence, we are back to the case 1, and the final formula only differs by a phase $(-1)^{2j_1}$.

3. **Case** $\omega_{k_1}^{\{\sigma\}} \in [-\pi, 0]$. We will have again the tetrahedron $\text{tet}_{\{\sigma\}}$ where the internal angle at k_1 is

$$\theta_{k_1}^{\{\sigma\}} \stackrel{\text{def.}}{=} \pi + \omega_{k_1}^{\{\sigma\}}, \quad (34)$$

Using the symmetries of Wigner matrices, we find that the relevant matrix element of the SU(2) rotation is

$$D_{\mu\nu}^{(j_1)}(e^{-\frac{i}{2}\phi_1\sigma_y} e^{-\frac{i}{2}\omega_{k_1}^{\{\sigma\}}\sigma_z} e^{-\frac{i}{2}\phi_n\sigma_y}) = e^{i\pi j_1} D_{-\mu\nu}^{(j_1)}\left(e^{-\frac{i}{2}\theta_{l_1}^{\{\sigma\}}\sigma_z} e^{-\frac{i}{2}(\pi-\varphi_{l_1, l_n}^{\{\sigma\}})\sigma_y} e^{-\frac{i}{2}(\pi-\theta_{l_n}^{\{\sigma\}})\sigma_z}\right). \quad (35)$$

4. **Case** $\omega_{k_1}^{\{\sigma\}} \in [\pi, 2\pi]$. The internal angle of $\text{tet}_{\{\sigma\}}$ is

$$\theta_{k_1}^{\{\sigma\}} \stackrel{\text{def.}}{=} -\pi + \omega_{k_1}^{\{\sigma\}}. \quad (36)$$

Following the reasoning of (33), we conclude that it differs from the case 3 only by a factor $(-1)^{2j_1}$.

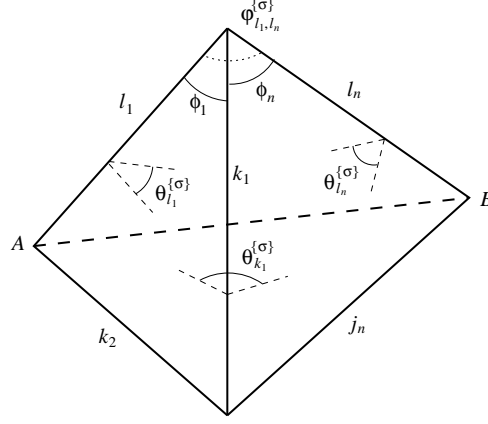


FIG. 7. Tetrahedron $\text{tet}_{\{\sigma\}}$ associated with a sign configuration $\{\sigma\}$. It is determined by the triangles (k_1, k_2, l_1) and (j_n, l_n, k_1) , and by the angle $\theta_{k_1}^{\{\sigma\}}$ between them, which in turn determine the length AB .

E. Final asymptotics formula

The above cases fit into a not-so-complicated formula.

$$\{3nj\} \approx \frac{(-1)^{r_n(\mathcal{E})}}{2^P \sqrt{d_{l_1} d_{l_n}}} \left[\prod_{p \in \mathcal{P}} \frac{1}{\sqrt{12\pi V_p}} \prod_{m \in \mathcal{E}} \frac{d_{\kappa_m}^{(l_m)}(\varphi_m)}{\sqrt{d_{j_m} d_{k_m}}} \right] \times \sum_{\{\sigma_p = \pm 1\}_{p \in \mathcal{P}}} \cos \left[\sum_{p \in \mathcal{P}} \sigma_p \left(S_R^{(p)} + \frac{\pi}{4} \right) + \pi(n+M)j_1 + f_{\mu\nu}^{\{\sigma\}} \right] d_{\mu\nu}^{(j_1)} \left(\phi_{l_1, l_n}^{\{\sigma\}} \right). \quad (37)$$

- \mathcal{P} is the set of tetrahedra on which the Ponzano-Regge formula has been applied, depicted in Figure 6, and $P = |\mathcal{P}|$. \mathcal{E} is the subset of $\{2, \dots, n-1\}$ corresponding to the small spins l_m , with $M = |\mathcal{E}|$. The global sign is given by $r_n(\mathcal{E}) = R_n + (n+M-1)(k_1+j_1) + (\mu-j_1) + (k_1+k_2+l_1) + (k_1+j_n+l_n) + \sum_{m \in \mathcal{E}} j_m + l_m + k_{m+1}$.
- $\mu = j_2 - l_1$ and $\nu = k_n - l_n$ are small, of the order of magnitude of j_1 . Also $\kappa_m = k_{m+1} - k_m$, $\eta_m = j_{m+1} - j_m$ are of order l_m for $m \in \mathcal{E}$.
- V_p and $S_R^{(p)}$ are the volumes and Regge actions of the tetrahedra tet_p , depicted in the Figure 6 and which have only large spins.
- To each sign configuration $\{\sigma\}$, we have assigned a tetrahedron $\text{tet}_{\{\sigma\}}$, Figure 7, defined by the gluing of the two triangles along k_1 with a dihedral angle $\theta_{k_1}^{\{\sigma\}}$ given in term of $\omega_{k_1}^{\{\sigma\}} = (n+M)\pi - \sum_{p \in \mathcal{P}} \sigma_p \Theta_{k_1}^{(p)}$ in the above subsection. The function $f_{\mu\nu}^{\{\sigma\}}$ depends on the value of $\omega_{k_1}^{\{\sigma\}}$ as follows,

$$f_{\mu\nu}^{\{\sigma\}} = \begin{cases} - (\mu\theta_{l_1}^{\{\sigma\}} + \nu\theta_{l_n}^{\{\sigma\}}) + 2\pi j_1 & \text{if } \omega_{k_1}^{\{\sigma\}} \in [-2\pi, -\pi], \\ (\mu\theta_{l_1}^{\{\sigma\}} + \nu\theta_{l_n}^{\{\sigma\}}) & \text{if } \omega_{k_1}^{\{\sigma\}} \in [-\pi, 0], \\ - (\mu\theta_{l_1}^{\{\sigma\}} + \nu\theta_{l_n}^{\{\sigma\}}) & \text{if } \omega_{k_1}^{\{\sigma\}} \in [0, \pi], \\ (\mu\theta_{l_1}^{\{\sigma\}} + \nu\theta_{l_n}^{\{\sigma\}}) + 2\pi j_1 & \text{if } \omega_{k_1}^{\{\sigma\}} \in [\pi, 2\pi]. \end{cases} \quad (38)$$

The angles $\varphi_{l_1, l_n}^{\{\sigma\}}$, $\theta_{l_1}^{\{\sigma\}}$, $\theta_{l_n}^{\{\sigma\}}$ are evaluated from the angles $\phi_1, \phi_n, \theta_{k_1}^{\{\sigma\}}$ following the Figure 7.

In our final result, there is a remaining sum over sign assignments $\{\sigma\}$. It is of combinatorial nature, and the initial sum over the intermediate spins x has been fully performed. Notice that the combinatorial sum contains *a priori* 2^P terms, but only 2^{P-1} are actually different. This sum assigns different frequencies to the oscillations, since in particular it sums over the Regge actions of individual tetrahedra with all possible signs. That phenomenon has also been observed in [26], where the authors looked at the asymptotics of the Ponzano-Regge model for 3d gravity on handlebodies and found a sum over ‘immersions’ with different frequencies like here.

III. EXAMPLES: ASYMPTOTICS OF 15J-SYMBOLS WITH SMALL AND LARGE ANGULAR MOMENTA

A simple example is obviously the 9j-symbol with a small spin, treated in the first section. It corresponds to the case where there is a single sum over $\sigma = \pm 1$, and $\omega_{k_1}^{(+)} \in [-2\pi, -\pi]$.

We now derive an asymptotic formula for the 15j-symbol with three small angular momenta, producing an alternative to the formula of [10], and formulae when one, two, three and four small angular momenta. The latter are new to our knowledge. In particular, though the formulae derived in [10] look similar, they apply to different, non-equivalent choices of the small spins.

Using the notation of [29], we have

$$\left\{ \begin{matrix} j_1 & j_2 & j_3 & j_4 & j_5 \\ l_1 & l_2 & l_3 & l_4 & l_5 \\ k_1 & k_2 & k_3 & k_4 & k_5 \end{matrix} \right\} = \sum_x d_x (-1)^{R_5} \left\{ \begin{matrix} j_1 & k_1 & x \\ k_2 & j_2 & l_1 \end{matrix} \right\} \left\{ \begin{matrix} j_2 & k_2 & x \\ k_3 & j_3 & l_2 \end{matrix} \right\} \left\{ \begin{matrix} j_3 & k_3 & x \\ k_4 & j_4 & l_3 \end{matrix} \right\} \\ \times \left\{ \begin{matrix} j_4 & k_4 & x \\ k_5 & j_5 & l_4 \end{matrix} \right\} \left\{ \begin{matrix} j_5 & k_5 & x \\ j_1 & k_1 & l_5 \end{matrix} \right\}, \quad (39)$$

where $R_5 = \sum_{i=1}^5 j_i + k_i + l_i$. In what follows, we always assume that j_1 is small. Thus, every other small spin must be chosen among l_2, l_3 and l_4 (see subsection II B).

1. Four small angular momenta

Assume that j_1, l_2, l_3 and l_4 are small. According to the notations of this section, we have

$$\mathcal{E} = \{2, 3, 4\} \quad \text{and} \quad \mathcal{P} = \emptyset. \quad (40)$$

It is easy to see from the derivation of (37) that if $\mathcal{P} = \emptyset$ then there is no sum over combinatorial sign assignments, $\{\sigma\} = \{0\}$. The corresponding tetrahedron $\text{tet}_{\{\sigma\}}$ is flattened to a triangle with $\varphi_{l_1, l_5} = \phi_1 + \phi_5$. The reason is that in the decomposition (39), all 6j-symbols have one small spin, so that no Ponzano-Regge formula gets involved. Consequently, there are no oscillations with some Regge action. Applying directly the general formula leads to

$$\{15j\} = \frac{(-1)^{j_1 + \mu}}{\sqrt{d_{l_1} d_{l_5} d_{j_2} d_{k_2} d_{j_3} d_{k_3} d_{j_4} d_{k_4}}} d_{\kappa_2 \eta_2}^{(l_2)}(\varphi_2) d_{\kappa_3 \eta_3}^{(l_3)}(\varphi_3) d_{\kappa_4 \eta_4}^{(l_4)}(\varphi_4) d_{\mu \nu}^{(j_1)}(\phi_1 + \phi_5), \quad (41)$$

with $\kappa_m \stackrel{\text{def.}}{=} k_{m+1} - k_m, \eta_m \stackrel{\text{def.}}{=} j_{m+1} - j_m, \mu \stackrel{\text{def.}}{=} j_2 - l_1$, and $\nu \stackrel{\text{def.}}{=} k_5 - l_5$.

That expression can be simplified. Since l_2, l_3 and l_4 are small, we have $j_2 \approx j_3 \approx j_4 \approx j_5$, and $k_2 \approx k_3 \approx k_4 \approx k_5$. Thus the triangles $(j_m, k_m, k_1)_{m \in \mathcal{E}}$, (k_1, j_2, k_2) , and (k_1, j_5, k_5) defined in Figure 5 are identical. Consequently, we have $\varphi_2 \approx \varphi_3 \approx \varphi_4 \approx \pi - \phi_1 - \phi_5$. The last (approximate) equality is simply due to the fact that the sum of the angles in a triangle is equal to π . The situation is illustrated in the Figure 8.

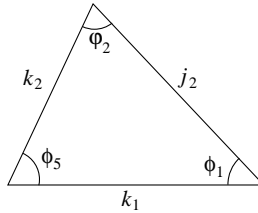


FIG. 8. Triangle defining the relevant geometric quantities for the asymptotics of the 15j-symbol with four small angular momenta.

This finally leads to

$$\{15j\} \approx \frac{1}{d_{j_2}^2 d_{k_2}^2} d_{\kappa_2 \eta_2}^{(l_2)}(\varphi_2) d_{\kappa_3 \eta_3}^{(l_3)}(\varphi_2) d_{\kappa_4 \eta_4}^{(l_4)}(\varphi_2) d_{\mu(-\nu)}^{(j_1)}(\varphi_2). \quad (42)$$

In [10], Yu gives an expression for the asymptotics of the 15j-symbol with four small spins chosen among the five l_i . Although this configuration is different from ours, both formulae look quite similar.

2. Three small angular momenta

We assume that j_1 , l_2 , and l_3 are small. The set of 6j-symbols on which we apply the Edmonds' and Ponzano-Regge formulae are

$$\mathcal{E} = \{2, 3\} \quad \text{and} \quad \mathcal{P} = \{4\}. \quad (43)$$

There are 2 sign configurations, $\sigma_4 = \pm$, that we denote respectively (+) and (-). Their contribution in the combinatorial sum are equal, so we consider only the (+) situation. The formula, once simplified, is

$$\{15j\} \approx \frac{(-1)^{k_1+j_4+l_4+k_5+2j_1+\mu}}{d_{j_2} d_{k_2} 12\pi V_4 \sqrt{d_{j_2} d_{k_5}}} d_{\kappa_2 \eta_2}^{(l_2)}(\varphi_2) d_{\kappa_3 \eta_3}^{(l_3)}(\varphi_2) d_{\mu\nu}^{(j_1)}(\varphi_{j_4, k_5}^{(+)}) \cos\left(S_R^{(4)} + \frac{\pi}{4} - \mu\theta_{j_4}^{(+)} - \nu\theta_{k_5}^{(+)} + j_1\pi\right), \quad (44)$$

where $\varphi_2 (\approx \varphi_3)$ is defined as usual; V_4 and $S_R^{(4)}$ are the volume and the Regge action of tet_4 , given in the Figure 9(a); and the angles $\varphi_{l_1, l_5}^{(+)}$, $\theta_{l_1}^{(+)}$ and $\theta_{l_5}^{(+)}$ belong to $\text{tet}_{(+)}$, represented in the Figure 9(b). The latter is built by gluing the triangles (k_1, l_1, k_2) , (k_1, l_5, j_5) with the dihedral angle $\theta_{k_1}^{(+)} \stackrel{\text{def.}}{=} \pi - \theta_{k_1}^{(4)}$, i.e. the external dihedral angle of tet_4 .

The attentive reader may have noticed that the tetrahedron $\text{tet}_{(+)}$ includes the triangle (j_4, k_4, k_1) whereas for the general case ($\text{tet}_{\{\sigma\}}$, in Figure 7), we used (l_1, k_2, k_1) instead. Both are actually equivalent since $j_4 \approx j_3 \approx j_2$ and $k_4 \approx k_3 \approx k_2$. Here, we have used that triangle to make contact with tet_4 .

The tetrahedron $\text{tet}_{(+)}$ is built out of the tetrahedron tet_4 in exactly the same way the second tetrahedron (named tet_2) was built from the first tetrahedron in the case of the 9j-symbol with one small spin. Indeed, one flips one of the two triangles which share k_1 , and set the external angle $\Theta_{k_1}^{(4)}$ as the new internal angle.

The underlying reason is that for the 9j-symbol with one small spin, just like for the 15j-symbol with three small spins and for any $3nj$ -symbol with $(n-2)$ small spins (chosen according to the hypotheses of Section II B), one makes use of a single Ponzano-Regge asymptotics formula. Therefore only one tetrahedron with large angular momenta is involved with dihedral angle θ_{k_1} at k_1 , and $\omega_{k_1}^{(+)} = 2\pi(n-2) + \theta_{k_1}$. Studying the range of $\omega_{k_1}^{(+)}$, one finds that the internal angle at k_1 in $\text{tet}_{(+)}$ is always $\theta_{k_1}^{(+)} = \pi - \theta_{k_1}^{(4)}$, i.e. the external angle of the reference tetrahedron. That means that the second tetrahedron is just built out of the first by the process we described.

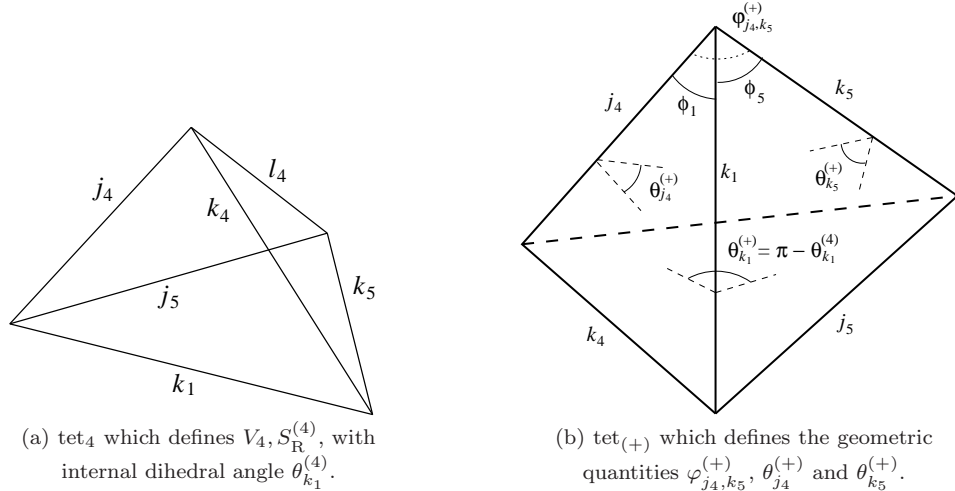


FIG. 9. Tetrahedra tet_4 and $\text{tet}_{(+)}$.

In [10], Yu has obtained an asymptotic formula for the 15j-symbol with j_1, l_3, l_4 being small. In that case, the tetrahedron of reference on which we have to apply the Ponzano-Regge formula is $\text{tet}_{p=2}$ from the Figure 6. However, Yu used a slightly different tetrahedron, which makes the formula a bit more complicated in the sense that one cannot express all the needed angles as angles from two tetrahedra only. Consequently the relevant Regge action is not the same as ours. Once the difference between the Regge actions is taken into account, it is possible to go from our formula to his' and to recover the geometric interpretation of his variables.

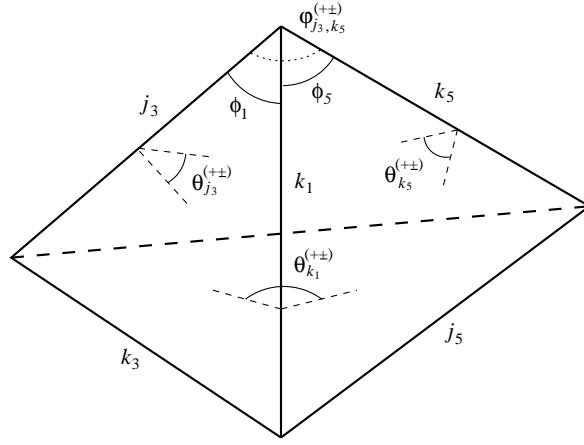


FIG. 10. Tetrahedra $\text{tet}_{(++)}$, $\text{tet}_{(+-)}$ which are defined by the angles ϕ_1, ϕ_5 and $\theta_{k_1}^{(+\pm)} = \pi - (\theta_{k_1}^{(3)} \pm \theta_{k_1}^{(4)})$. They define in turn the angles $\varphi_{j_3, k_5}^{(+\pm)}, \theta_{j_3}^{(+\pm)}$ and $\theta_{k_5}^{(+\pm)}$.

3. Two small angular momenta

We assume that j_1 and l_2 are small. The set of 6j-symbols on which we apply the Edmonds' and Ponzano-Regge formulae are

$$\mathcal{E} = \{2\} \quad \text{and} \quad \mathcal{P} = \{3, 4\}. \quad (45)$$

There are $2^2 = 4$ sign configurations, $(\sigma_3, \sigma_4) = (++)$, $(+-)$, $(-+)$, $(--)$. Thanks to the symmetry of the combinatorial sum, we can consider only the cases $(+\pm)$.

We now have two tetrahedra, tet_3 and tet_4 , with large angular momenta as in Figure 6 for $p = 3, 4$. To avoid distinguishing behaviors depending on their dihedral angles, we assume that they are nearly regular, so that their angles are close to $\theta_{\text{reg}} = \arccos 1/3$. Also we assume without loss of generality that $\theta_{k_1}^{(3)} - \theta_{k_1}^{(4)} \geq 0$.

The asymptotic formula is then

$$\{15j\} \approx \frac{(-1)^{j_3+l_3+j_4+k_4+l_4+k_5+j_1+\mu+2k_1}}{24\pi d_{j_3} \sqrt{d_{k_3} d_{k_5} V_3 V_4}} d_{\kappa_2 \eta_2}^{(l_2)}(\varphi_2) \left[-d_{\mu\nu}^{(j_1)}(\varphi_{j_3, k_5}^{(++)}) \sin \left(S_{\text{R}}^{(3)} + S_{\text{R}}^{(4)} - \mu\theta_{j_3}^{(++)} - \nu\theta_{k_5}^{(++)} \right) \right. \\ \left. + (-1)^{2j_1} d_{\mu\nu}^{(j_1)}(\varphi_{j_3, k_5}^{(+-)}) \cos \left(S_{\text{R}}^{(3)} - S_{\text{R}}^{(4)} - \mu\theta_{j_3}^{(+-)} - \nu\theta_{k_5}^{(+-)} \right) \right]. \quad (46)$$

The volumes V_3, V_4 and Regge actions $S_{\text{R}}^{(3)}, S_{\text{R}}^{(4)}$ are associated with the tetrahedra $\text{tet}_3, \text{tet}_4$, see Figure 6. The angles $\varphi_{j_3, k_5}^{(+\pm)}, \theta_{j_3}^{(+\pm)}$ and $\theta_{k_5}^{(+\pm)}$ are defined in Figure 10 which pictures $\text{tet}_{(+\pm)}$.

Let us explain how to get the secondary tetrahedra $\text{tet}_{(+\pm)}$. Notice that tet_3 and tet_4 have a common triangle, (k_1, j_4, k_4) . Hence they can be glued together, in two different ways, either from the outside or one inside the other. We remove the common triangle (k_1, j_4, k_4) so that the angle at k_1 between (k_1, j_3, k_3) and (k_1, j_5, k_5) is either $\theta_{k_1}^{(3)} + \theta_{k_1}^{(4)}$, or $\theta_{k_1}^{(3)} - \theta_{k_1}^{(4)}$.

The generic study tells us to consider the angle $\omega_{k_1}^{(+\pm)} \stackrel{\text{def.}}{=} 6\pi - \Theta_{k_1}^{(3)} \mp \Theta_{k_1}^{(4)}$. One gets

$$\omega_{k_1}^{(+\pm)} = \theta_{k_1}^{(3)} \pm \theta_{k_1}^{(4)} - (1 \mp 1)\pi \pmod{4\pi}, \quad (47)$$

which implies $\omega_{k_1}^{(++)} \in [0, \pi]$ and $\omega_{k_1}^{(+-)} \in [-2\pi, -\pi]$. As a conclusion, the tetrahedra $\text{tet}_{(+\pm)}$ are built by flipping the triangle (k_1, j_5, k_5) so that k_5 meet j_3 while j_5 meet k_3 . Then from those five lengths, get a tetrahedron by setting as the new dihedral angle at k_1

$$\theta_{k_1}^{(+\pm)} = \pi - (\theta_{k_1}^{(3)} \pm \theta_{k_1}^{(4)}), \quad (48)$$

like in Figure 10.

In [10] a formula for the 15j-symbol with two small angular momenta is given, which are l_3, l_4 . That configuration is not the same as here, but the formulae look quite similar. A notable difference is the denominator of the amplitude which is here the product of the volumes of the two relevant tetrahedra, while it is more complicated in [10].

4. One small angular momentum

We assume that only j_1 is small. The set of 6j-symbols on which we apply the Edmonds' and Ponzano-Regge formulae are

$$\mathcal{E} = \emptyset \quad \text{and} \quad \mathcal{P} = \{2, 3, 4\}. \quad (49)$$

There are $2^3 = 8$ sign configurations $(\sigma_2, \sigma_3, \sigma_4)$. Thanks to the symmetry of the combinatorial sum, we can consider only $(+++)$ and $(++-), (+-+), (-++)$.

For simplicity, we assume that the three tetrahedra associated to \mathcal{P} are almost regular. We get

$$\begin{aligned} \{15j\} \approx & \frac{(-1)^{(j_2+l_2+j_3)+(k_3+l_3+k_4)+j_4+l_4+k_5-k_1+\mu}}{48\pi\sqrt{12\pi d_{j_2}d_{k_2}V_2V_3V_4}} \\ & \left[d_{\mu\nu}^{(j_1)}(\varphi_{j_2,k_5}^{(++-)}) \cos\left(S_R^{(2)} + S_R^{(3)} - S_R^{(4)} + \frac{\pi}{4} - \mu\theta_{j_2}^{(++-)} - \nu\theta_{k_5}^{(++-)} + \pi j_1\right) \right. \\ & + d_{\mu\nu}^{(j_1)}(\varphi_{j_2,k_5}^{(+-+)})) \cos\left(S_R^{(2)} - S_R^{(3)} + S_R^{(4)} + \frac{\pi}{4} - \mu\theta_{j_2}^{(+-+)} - \nu\theta_{k_5}^{(+-+)} + \pi j_1\right) \\ & + d_{\mu\nu}^{(j_1)}(\varphi_{j_2,k_5}^{(-++)}) \cos\left(-S_R^{(2)} + S_R^{(3)} + S_R^{(4)} + \frac{\pi}{4} - \mu\theta_{j_2}^{(-++)} - \nu\theta_{k_5}^{(-++)} + \pi j_1\right) \\ & \left. + d_{\mu\nu}^{(j_1)}(\varphi_{j_2,k_5}^{(+++)}) \cos\left(S_R^{(2)} + S_R^{(3)} + S_R^{(4)} + \frac{3\pi}{4} + \mu\theta_{j_2}^{(+++)} + \nu\theta_{k_5}^{(+++)} + \pi j_1\right) \right]. \quad (50) \end{aligned}$$

The volumes V_3, V_4, V_5 and Regge actions $S_R^{(2)}, S_R^{(3)}, S_R^{(4)}$ are associated with the tetrahedra $\text{tet}_2, \text{tet}_3, \text{tet}_4$, respectively, see the Figure 6 for $p = 2, 3, 4$. The angles $\varphi_{j_2,k_5}^{(\pm\pm\pm)}, \theta_{j_2}^{(\pm\pm\pm)}$ and $\theta_{k_5}^{(\pm\pm\pm)}$ belong to the tetrahedra $\text{tet}_{(\pm\pm\pm)}$. They are defined by the five spins k_1, j_2, k_2, j_5, k_5 which form two triangles glued along k_1 like in Figure 11. To complete their definition, we set the dihedral angle at k_1 to be

$$\begin{aligned} \theta_{k_1}^{(+++)} &= \theta_{k_1}^{(2)} + \theta_{k_1}^{(3)} + \theta_{k_1}^{(4)} - \pi, \\ \theta_{k_1}^{(++-)} &= \pi - \theta_{k_1}^{(2)} - \theta_{k_1}^{(3)} + \theta_{k_1}^{(4)}, \\ \theta_{k_1}^{(+-+)} &= \pi - \theta_{k_1}^{(2)} + \theta_{k_1}^{(3)} - \theta_{k_1}^{(4)}, \\ \theta_{k_1}^{(-++)} &= \pi + \theta_{k_1}^{(2)} - \theta_{k_1}^{(3)} - \theta_{k_1}^{(4)}. \end{aligned} \quad (51)$$

Note that since $\text{tet}_2, \text{tet}_3, \text{tet}_4$ are close to being regular the above angle indeed lie in $[0, \pi]$.

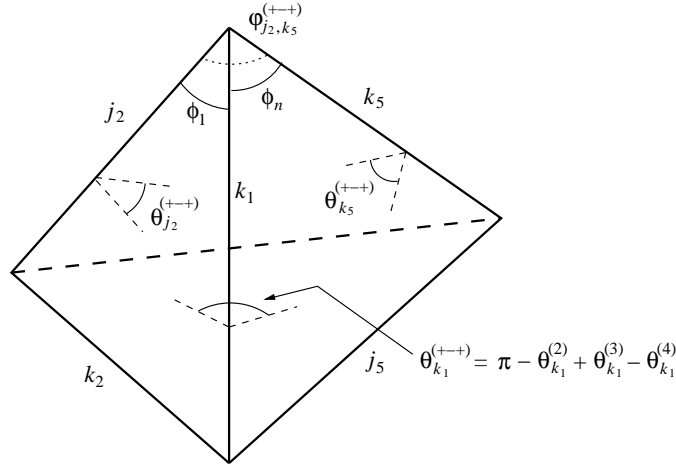


FIG. 11. Tetrahedron $\text{tet}_{(+--+)}$ which defines the geometric quantities $\varphi_{j_2,k_5}^{(+--+)}, \theta_{j_2}^{(+--+)}$ and $\theta_{k_5}^{(+--+)}$, given ϕ_1, ϕ_5 and $\theta_{k_1}^{(+--+)}$.

The intuitive way of building those tetrahedra is by first gluing $\text{tet}_2, \text{tet}_3$ along their common triangle (k_1, j_3, k_3) . There are two different ways, either on the outside, or one inside the other. Then, one adds tet_4 by gluing it along the triangle (k_1, j_4, k_4) , and there are here again two different ways to do so. Finally we focus on the triangles (k_1, j_2, k_2) and (k_1, j_5, k_5) which can be completed to a tetrahedron, and we consider the tetrahedron which complements that one when drawing the parallelogram spanned by (j_2, k_2) . The final internal angle is given by (51), depending on the chosen way to glue the three initial tetrahedra. As an example, we give $\text{tet}_{(+--+)}$ in Figure 11.

IV. CONCLUSION

We have shown that the result of [8] can be recovered by direct application of the Ponzano-Regge formula (together with Edmonds' formula), making clear the way the asymptotic information is encoded into the geometry of a tetrahedron. Moreover, the conditions of applicability of our method have been given and we derived new, explicit formulae for asymptotics of arbitrary Wigner symbols with some large and small angular momenta. Our method is simpler than that of [8], as far as Wigner symbols are concerned, and provides us with complementary results.

Some directions for future research are proposed in the Conclusion of [8] and are definitely of interest.

We would like to mention in addition that beyond the asymptotic formulae for specific symbols, the regime where some spins remain small should deserve attention, because the geometric content is simply contained in tetrahedra. In particular, it may be investigated in terms of recurrence relations. As argued in [30], the latter provides a preferred way to encode the geometric properties of classical spin networks. It was further shown in [22], in the case of the 6j-symbol, that it is possible to derive those recurrences as quantum constraints (Wheeler-DeWitt equations) coming from three-dimensional gravity. The same result holds in the four-dimensional context [27] using a Hamiltonian from topological field theory. Hence, it would be interesting to look at the asymptotics of those relations with small and large spins, and to look for a similar regime where the asymptotic geometry is described in terms of 4-simplexes instead of tetrahedra.

ACKNOWLEDGEMENTS

P.F. acknowledges the Summer Program of Perimeter Institute for undergraduate students, without which this project could have been completed.

Research at Perimeter Institute is supported by the Government of Canada through Industry Canada and by the Province of Ontario through the Ministry of Research and Innovation.

-
- [1] V. Aquilanti, A. C. P. Bitencourt, C. d. S. Ferreira, A. Marzuoli and M. Ragni, "Quantum and semiclassical spin networks: From atomic and molecular physics to quantum computing and gravity," *Phys. Scripta* **78**, 058103 (2008) [arXiv:0901.1074 [quant-ph]].
 - [2] M. Carfora, A. Marzuoli and M. Rasetti, "Quantum Tetrahedra," *J. Phys. Chem. A* **113**, 15367 (2009) [arXiv:1001.4402 [math-ph]].
 - [3] M. A. Levin and X. G. Wen, "String net condensation: A Physical mechanism for topological phases," *Phys. Rev. B* **71**, 045110 (2005) [arXiv:cond-mat/0404617].
 - [4] K. Noui and A. Perez, "Three-dimensional loop quantum gravity: Physical scalar product and spin foam models," *Class. Quant. Grav.* **22**, 1739 (2005) [arXiv:gr-qc/0402110].
 - [5] J. C. Baez, "An Introduction to spin foam models of quantum gravity and BF theory," *Lect. Notes Phys.* **543**, 25 (2000) [arXiv:gr-qc/9905087].
 - [6] L. Freidel and K. Krasnov, "Spin foam models and the classical action principle," *Adv. Theor. Math. Phys.* **2**, 1183 (1999) [arXiv:hep-th/9807092].
 - [7] L. Freidel and D. Louapre, "Ponzano-Regge model revisited I: Gauge fixing, observables and interacting spinning particles," *Class. Quant. Grav.* **21**, 5685 (2004) [arXiv:hep-th/0401076].
 - [8] R. G. Littlejohn and L. Yu, "Semiclassical Analysis of the Wigner 9J-Symbol with Small and Large Angular Momenta," *Phys. Rev. A* **83** (2011) 052114 [arXiv:1104.1499 [math-ph]].
 - [9] L. Yu, "Semiclassical Analysis of the Wigner 12J-Symbol with One Small Angular Momentum: Part I," arXiv:1104.3275 [math-ph].
 - [10] L. Yu, "Asymptotic Limits of the Wigner 15J-Symbol with Small Quantum Numbers," arXiv:1104.3641 [math-ph].
 - [11] K. Schulten and R. G. Gordon, "Semiclassical approximations to 3J and 6J coefficients for quantum mechanical coupling of angular momenta," *J. Math. Phys.* **16**:1971–1988, 1975.
 - [12] J. Roberts, "Classical 6j-symbols and the tetrahedron," *Geom. Topol.* **3** (1999), 21-6 [arXiv:math-ph/9812013].
 - [13] L. Freidel and D. Louapre, "Asymptotics of 6j and 10j symbols," *Class. Quant. Grav.* **20**, 1267 (2003) [arXiv:hep-th/0209134].
 - [14] R. Gurau, "The Ponzano-Regge asymptotic of the 6j symbol: An Elementary proof," *Annales Henri Poincare* **9**, 1413 (2008) [arXiv:0808.3533 [math-ph]].
 - [15] A. R. Edmonds, "Angular momentum in quantum mechanics," Princeton: Princeton University Press.
 - [16] J. P. M. Flude, "The Edmonds asymptotic formulas for the 3j and 6j symbols," *J. Math. Phys.* **39** 3906 (1998).
 - [17] V. Aquilanti, H. M. Haggard, A. Hedeman, N. Jeevanjee, R. G. Littlejohn and L. Yu, "Semiclassical Mechanics of the Wigner 6j-Symbol," arXiv:1009.2811 [math-ph].

- [18] V. Bonzom, E. R. Livine, M. Smerlak and S. Speziale, “Towards the graviton from spinfoams: The Complete perturbative expansion of the 3d toy model,” Nucl. Phys. B **804**, 507 (2008) [arXiv:0802.3983 [gr-qc]].
- [19] M. Dupuis and E. R. Livine, “Pushing Further the Asymptotics of the 6j-symbol,” Phys. Rev. D **80**, 024035 (2009) [arXiv:0905.4188 [gr-qc]].
- [20] M. Dupuis and E. R. Livine, “The 6j-symbol: Recursion, Correlations and Asymptotics,” Class. Quant. Grav. **27**, 135003 (2010) [arXiv:0910.2425 [gr-qc]].
- [21] V. Bonzom and E. R. Livine, “Yet Another Recursion Relation for the 6j-Symbol,” arXiv:1103.3415 [gr-qc].
- [22] V. Bonzom and L. Freidel, “The Hamiltonian constraint in 3d Riemannian loop quantum gravity,” arXiv:1101.3524 [gr-qc].
- [23] R. W. Anderson, V. Aquilanti and A. Marzuoli, “3nj Morphogenesis and Semiclassical Disentangling,” J. Phys. Chem. A **113** (2009) 15106. arXiv:1001.4386 [quant-ph].
- [24] J. W. Barrett, W. J. Fairbairn and F. Hellmann, “Quantum gravity asymptotics from the SU(2) 15j symbol,” Int. J. Mod. Phys. A **25** (2010), 2897–2916. [arXiv:0912.4907 [gr-qc]].
- [25] J. W. Barrett, R. J. Dowdall, W. J. Fairbairn, H. Gomes, F. Hellmann and R. Pereira, “Asymptotics of 4d spin foam models,” (2010). arXiv:1003.1886 [gr-qc].
- [26] R. J. Dowdall, H. Gomes and F. Hellmann, “Asymptotic analysis of the Ponzano-Regge model for handlebodies,” J. Phys. A **43**, 115203 (2010) [arXiv:0909.2027 [gr-qc]].
- [27] V. Bonzom, “Spin foam models and the Wheeler-DeWitt equation for the quantum 4-simplex,” Phys. Rev. D **84** 024009 (2011). arXiv:1101.1615 [gr-qc].
- [28] D. A. Varshalovich, A. N. Moskalev and V. K. Khersonsky, “Quantum theory of angular momentum: irreducible tensors, spherical harmonics, vector coupling coefficients, 3nj symbols,” *Singapore, Singapore: World Scientific (1988) 514p*
- [29] A. P. Yutsis, I. B. Levinson and V. V. Vanagas, “Mathematical apparatus of the theory of angular momentum,” (1962) *Israel Program for Scientific Translations*.
- [30] V. Bonzom, E. R. Livine and S. Speziale, “Recurrence relations for spin foam vertices,” Class. Quant. Grav. **27**, 125002 (2010) [arXiv:0911.2204 [gr-qc]].